Int. J. Electrochem. Sci., 7 **(2012)** 12846 - 12855

International Journal of ELECTROCHEMICAL SCIENCE
www.electrochemsci.org

Electrochemical Induced Codeposition of Li with Cu from 1-Hexyl-3-Methylimidazolium Trifluoromethanesulfonate Ionic Liquid

*Bo Yan, Jinqiu Zhang, Peixia Yang and Maozhong An**

State Key Laboratory of Urban Water Resource and Environment, School of Chemical Engineering and Technology, Harbin Institute of Technology, Harbin 150001, China
*E-mail: mzan@hit.edu.cn

Received: 17 October 2012 / *Accepted:* 10 November 2012 / *Published:* 1 December 2012

The cyclic voltammetric behavior of 1-hexyl-3-methylimidazolium trifluoromethanesulfonate (HMIMOTF) ionic liquid containing Li(I), Cu(II) and mixtures of Li(I) and Cu(II) was studied at 333 K. Induced codeposition model was developed to explain the codeposition of Li with Cu. The XRD results showed that Li exists as amorphous Li. The content of Li in the deposit could reach to 76.81 at% and Li distributed uniformly in mesh porous Cu framework that obtained by dissolving deposited Li in distilled water.

Keywords: ionic liquid, induced codeposition, Li-Cu deposit

1. INTRODUCTION

Electrodeposition is widely used to obtain protective coatings, decorative coatings and functional materials. The electrodeposition history is based solely on aqueous solutions due to its high solubility of metal salts, which results in highly conducting solutions.[1] However, as narrow electrochemical window of aqueous solutions, active metals, such as Li and Mg, can’t deposit from aqueous solutions since their negative reduction potential and the reaction between active metals and water. The main driving force for non-aqueous electrolytes has been the desire to deposit these active metals.

Room temperature ionic liquids (RTILs) have attracted much attention in electrodeposition of metal and alloys, such as Zn-Mn, Cu-Sn, Al-Ce and Cu-Mn, for their wide electrochemical window and thermal stability. [2-6] Thus, RTILs can be used as plating bath for reactive metals that are difficult to be deposited from aqueous system, such as Mg, Al, Se, Li and their alloys.[7-12]

Metallica lithium is thought to be an ideal anode for Li-ion batteries due to its high activity to realize high cell voltage.[13] However, the dendrite formation of Li metal during charging seriously limits large-scale application of Li-ion batteries. Polymer electrolytes and additives were used to suppress dendrite growth of Li.[14-19]

As low reactivity and excellent electrical properties of Cu in Li-ion batteries environment,[20] Cu framework of Li-Cu well inhibits the dendrite formation of Li metal during charging and Li-Cu deposit with high atom content of Li is expected to be an active anode material to improve the safety of Li-ion batteries. However, it is difficult to obtain Li-Cu deposit with high Li atom content because of low solubility of Li in pure Cu and large deposition potential difference between Li and Cu.[21] Cu-Li alloy with 18% atom content of Li was electrodeposited from a fused salt solution composed of LiCl and $CuCl_2$ at about 753K.[22]

In the present work a Li-Cu deposit with high atom content of Li was obtained by electrochemical codeposition from 1-hexyl-3-methylimidazolium trifluoromethanesulfonate (HMIMOTF) ionic liquid and an induced codeposition model was developed to explain the codeposition behavior of Li with Cu. Cu framework with mesh porous structure is obtained after dissolving Li in obtained Li-Cu deposit in distilled water. The obtained Cu framework with mesh porous structure is desired since its high surface area and porous structure which is shown to be advantageous for anode materials.[23] Meanwhile, the obtained Cu framework has an excellent inhibitory effect on the dendrite formation of Li metal as its low activity in Li-ion batteries environment.[20]

2. EXPRIMENT

2.1 Chemical and reagents

The ionic liquid HMIMOTF (Shanghai Chengjie Chemical Co., Ltd) was dried under vacuum for 24h at 373 K. Anhydrous $LiCF_3SO_3$ (Aladding, 99%) and anhydrous $Cu(CF_3SO_3)_2$ (Aladding, 99%) were dissolved in HMIMOTF separately or together to prepare electrolytes that were stirred for 24h at 333 K before electrodeposition or electrochemical testing. All the electrochemical experiments were carried out in an argon gas-filled glovebox with concentration of O_2 and H_2O <10ppm.

2.2 Measurement procedures and apparatus

In a conventional 3-electrode cell, a platinum foil with 1 cm^2 working area, a platinum plate and a platinum wire were used as the working electrode (WE), the counter electrode (CE) and the quasireference electrode (QRE), respectively. Cyclic voltammograms (CVs), potentiostatic electrolysis (electrodeposition under controlled potential) and constant current electrodeposition were carried out using a Princeton Applied Research Parstat 2273 potentiostat/galvanostat controlled by PowerSuite software. The deposits on the WE were washed in NMP to remove the ionic liquid residue in the glove box and then was analyzed by X-ray diffractometry (XRD, Philips，X'Pert diffractometer, CuKα radiation). The composition of the deposit was measured using inductively coupled plasma atomic emission spectrometry (ICP-AES, Perkin Elmer, 5300DV) after dissolving the deposit in a nitric acid aquatic solution. A field-emission scanning electron microscope (FE-SEM, Hitachi S4700) was used to characterize the surface morphologies of the deposit and the Cu framework obtained after dissolving Li of the deposit in distilled water. X-ray photoelectron spectroscopy (XPS) analysis was taken by PHI 5700 ESCA System with monochromatic Al Kα radiation (1486.6 eV). All spectra were calibrated so that the binding energy of the C 1s peaks was 284.6 eV. The absorption of ionic liquid containing 0.1M $Cu(CF_3SO_3)_2$ and 1M $LiCF_3SO_3$+0.1M $Cu(CF_3SO_3)_2$ were measured using an air-tight quartz cell (light path length 1mm) with the aid of UV-vis spectrometer (Shimazu, UV-2550).

3. RESULTS AND DISCUSSION

Fig. 1 shows CVs on Pt WE in HMIMOTF, HMIMOTF containing 0.1M $Cu(CF_3SO_3)_2$, 1M $LiCF_3SO_3$, and 0.1M $Cu(CF_3SO_3)_2$ + 1M $LiCF_3SO_3$, respectively. Fig. 1a indicates that the electrochemical window of HMIMOTF is around 4.2 V (from 2~ -2.2 V *vs*. Pt). The cathodic and anodic currents in Fig. 1a are due to the decomposition of $HMIM^+$ and the oxidation of the reduction product of $HMIM^+$. Fig 1b reveals that a two-step two-electron reduction of Cu^{2+} to Cu occurs in HMIMOTF containing 0.1M $Cu(CF_3SO_3)_2$ as two reduction peaks at about -0.3 and -0.5V are observed, respectively. And two oxidation peaks at about -0.1 and 0 V are observed clearly which correspond to $Cu \rightarrow Cu^+$ and $Cu^+ \rightarrow Cu^{2+}$, respectively. No reduction peak is found in the electrolyte of HMIMOTF containing 1M $LiCF_3SO_3$, as shown in Fig. 1c, indicating that Li can't deposit solely from HMIMOTF. Interestingly, two reduction peaks at about –2.7 V and -4.4 V corresponding to under potential deposition (UPD) and deposition of Li are observed clearly in Fig. 1d, indicating that Li can be codeposited with addition of $Cu(CF_3SO_3)_2$ in HMIMOTF. Meanwhile, the cathodic current of the electrolyte containing 1M $LiCF_3SO_3$ and $Cu(CF_3SO_3)_2$ is smaller than that of HMIMOTF containing only 1M $LiCF_3SO_3$, which is due to the formation of solid electrolyte interphase (SEI). The SEI, immediately formed by deposited Li contacting with electrolyte, is a passivation film which is thought to be where the deposition/dissolution of lithium taking place and prevents the decomposition of electrolyte.[24,25]

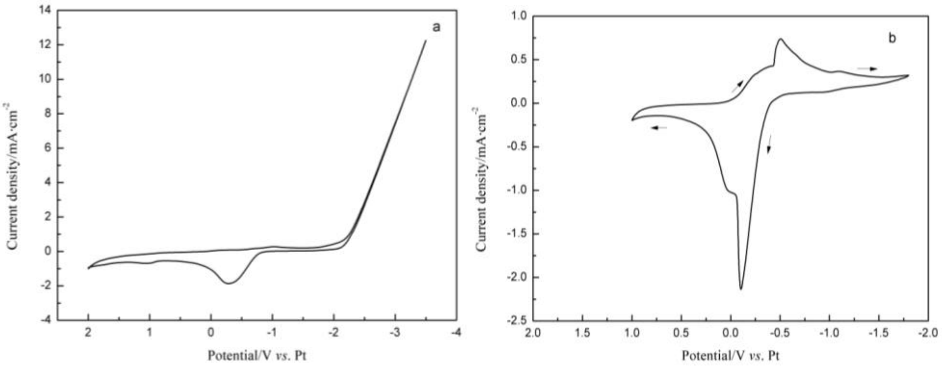

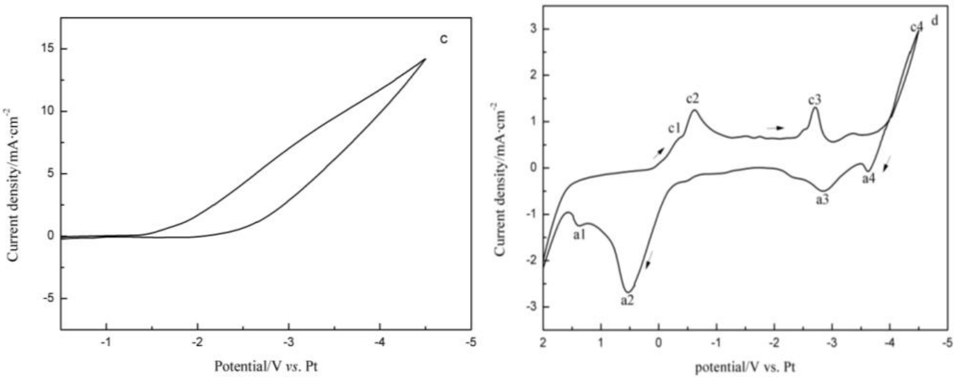

Figure 1. a) CVs on Pt WE in HMIMOTF, b) HMIMOTF containing 0.1M $Cu(CF_3SO_3)_2$, c) 1M $LiCF_3SO_3$, and d) 0.1M $Cu(CF_3SO_3)_2$ + 1M $LiCF_3SO_3$. Scan rate: 50mv/s.

The behavior of codeposition of Li with Cu from HMIMOTF can be explained by induced deposition. The induced deposition is a special case of anomalous codeposition, which is thought to be that the more difficult-to-deposit metal deposit from an insoluble film on the surface of electrode rather than by reduction of ions in solution. If the insoluble film is conducting and completely blocks all solutions ions from being reduced at the electrode, one could deposit an alloy of the two metals in a fixed atom ratio. Otherwise if the insoluble film is conducting but doesn't completely block all solution ions from being reduced one obtains deposits that reflect both the composition of the film and the composition of solution[26]. An induced codeposition model is developed to explain the codeposition of Li with Cu in this system, as illustrated in Fig. 2, Cu ions and Li ions formed an insoluble film on the surface of the electrode and then Cu deposited on the surface of Pt electrode at the beginning of deposition since Cu ions have more positive deposit polarization than Li ions. Part of energy releases during the nucleation process of Cu ions and this energy gathers on the surface of Pt electrode which increased potential of electrode [27]. Thus, the polarization decreased which makes it easier for Li to deposit on the electrode.

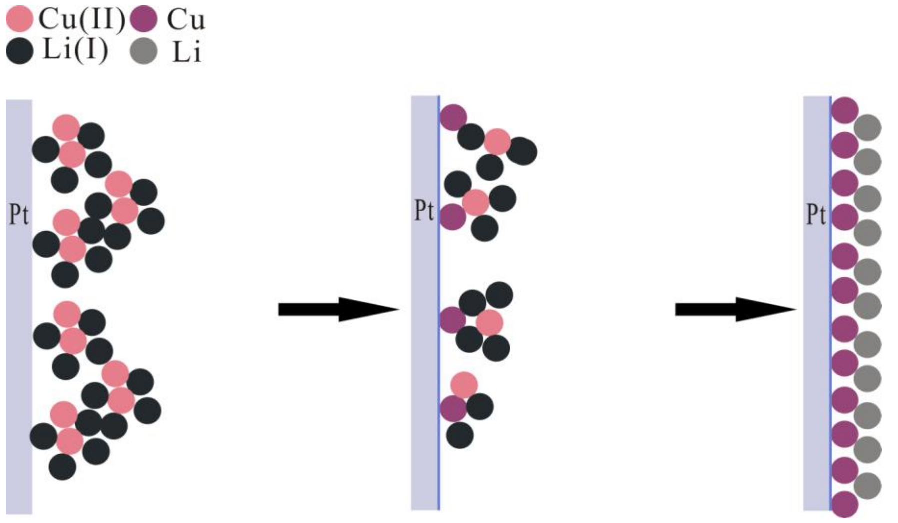

Figure 2. Model of induced codepostion

In order to confirm the above mechanism, potentiostatic electrolysis with different molar ratio of 1:1 (Li:Cu), 2.5:1, 5:1, 7.5:1 and 10:1 were carried out for 4h at -4.0 V with a temperature of 333 K, the composition of deposits obtained at different molar ratio were shown in Table 1. Table 1 indicates that the atom content of Li in Li-Cu deposit increased with the increasing of concentration of Li ions in the electrolyte, which means that the insoluble compound formed during induced deposition didn't block all the solutions ions from being reduced so the obtained Li-Cu deposit reflect both the composition of the compound and the composition of solution. Fig. 3 shows the absorption of ionic liquid containing 0.1M $Cu(CF_3SO_3)_2$ and 1M $LiCF_3SO_3$+0.1M $Cu(CF_3SO_3)_2$. The absorption peaks in both a and b were due to the addition of Cu ions into ionic liquid since the basic line was made by neat ionic liquid. No difference was found between the spectra before and after the addition of $LiCF_3SO_3$, indicating that $LiCF_3SO_3$ and $Cu(CF_3SO_3)_2$ dispersed separately in ionic liquid since if $LiCF_3SO_3$ and $Cu(CF_3SO_3)_2$ formed new compound the absorption peak of $Cu(CF_3SO_3)_2$ would change.

Table 1. the composition of deposits obtained at different molar ratio

Concentration of Li ions	Concentration of Cu ions	Atom content of Li（at%）
0.1M	0.1M	18.72%
0.25M	0.1M	33.67%
0.5M	0.1M	57.90%
0.75M	0.1M	58.65%
1M	0.1M	76.81%

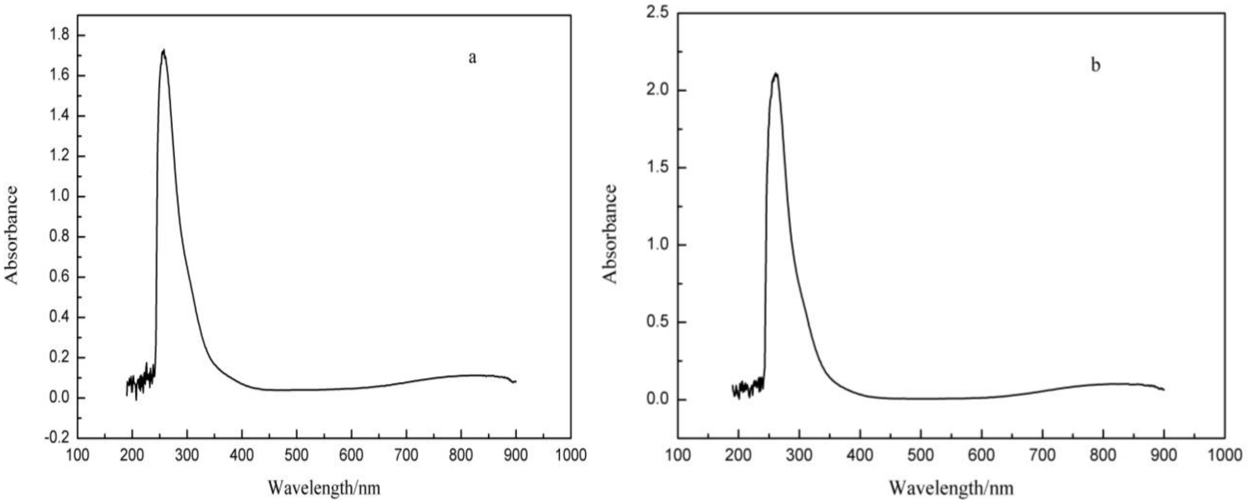

Figure 3. UV–vis spectra obtained in HMIMOTF containing (a) 0.1M $Cu(CF_3SO_3)_2$ and (b) 1M $LiCF_3SO_3$+0.1M $Cu(CF_3SO_3)_2$

An E-t curve, as illustrated in Fig. 4, was obtained to record the change of potential with time during a constant current electrodeposition which was carried out at current density of 0.5mA/cm^2 for

1h. Three small arrows a, b, and c are plotted to mark the reduction of Cu ions, decomposition of HMIMOTF, and codeposition of Li, respectively. Before deposition, the potential of Pt electrode is 0V. When deposition starts, the potential drops rapidly. But, at 22 s, as marked by arrow a, the potential slowly dropped down from -0.53V to -1V, indicating the reduction procedure of Cu ions. With time increasing, the potential is continuing to drop to -2.1V at a rapid speed. A short potential plat within a timescale of about 60s is observed at the position of arrow b, implying the decomposition of HMIMOTF. Then the potential still dropped rapidly to the position marked by arrow c, where the potential begins slowly dropping to -4V and keeping at -4V during the rest deposition treatment, indicating codeposition of Li with Cu. The E-t curve well confirms the assumption about induced deposition and has a good agreement with CV of HMIMOTF containing 0.1M $Cu(CF_3SO_3)_2$ and 1M $LiCF_3SO_3$.

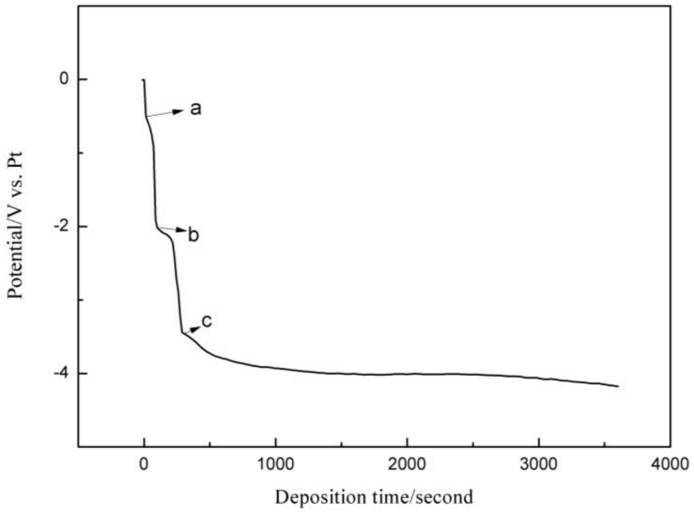

Figure 4. E-t curve of HMIMOTF containing 0.1M $Cu(CF_3SO_3)_2$ + 1M $LiCF_3SO_3$. Current density: 0.5mA/cm^2

Potentiostatic electrolysis were carried out at -2.5V, -3.0V, -3.5V and -4.0V for 4h at 333 K. In order to obtain a higher atom content of Li, the concentration of Li ions and Cu ions chosen here were 1M and 0.1M, respectively. Black deposits were obtained on Pt substrate after the electrolysis. The composition of Li-Cu deposits and coulombic efficiency obtained at different potential was shown in Table 2. The atom content of Li in Li-Cu deposit was 39.82% when the deposition potential was -2.5V and the total coulombic efficiency was 18.97%. This result was rather reasonable because this potential was far beyond the deposition of Cu ions and the decomposition of ionic liquid but much more positive to the deposition potential of Li ions, which made the total coulombic efficiency very low as the decomposition of ionic liquid was the main reaction under this potential. When the deposition potential moved to -3.0V the atom content of Li increased to 68.84%. Furthermore, the coulombic efficiency increased to 30.01% at the same time. The increasing of coulombic efficiency may due to the increasing of atom content of Li in Li-Cu deposit which leads to the formation of SEI film. Although the atom content of Li increased to 76.81% when the deposition moved to -3.5V, the coulombic efficiency decreased to 27.70% as the decomposition of ionic liquid was much more seriously under this deposition potential. When the deposition moved to -4.0V both the atom content of Li and coulombic efficiency decreased for the serious decomposition of ionic liquid.

Table 2. The composition of Li-Cu deposits and coulombic efficiency obtained at different potential

Deposition potential	Atom content of Li	Coulombic efficiency
-2.5V	39.82	18.97%
-3.0V	68.84	30.01%
-3.5V	76.81	27.70%
-4.0V	70.85	24.30%

Only 76.81at% (atom content of Li in Li-Cu deposit) Li-Cu deposit was chosen for further study due to its high Li atom content. By comparison of XRD patterns of Pt substrate and 76.81at%Li-Cu deposit as shown in Fig. 5a and b, sharp diffraction peaks at 2θ=39.75°, 46.23°, 67.45°, 81.24°, 85.69° in both patterns are attributed to Pt substrate. In Fig. 2b, the peak at 2θ=43.34° relate to reflection (111) of Cu.

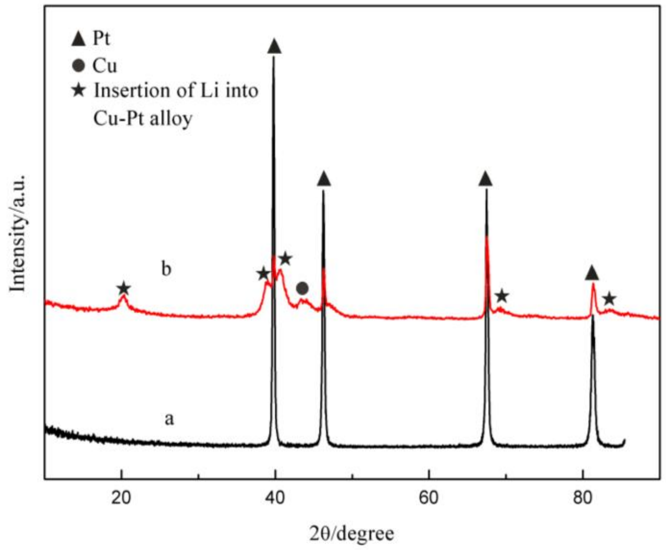

Figure 5. XRD patterns of a) Pt substrate and b) Li-Cu deposit on Pt WE in HMIMOTF containing 0.1M $Cu(CF_3SO_3)_2$ and 1M $LiCF_3SO_3$ at -3.5V (vs. Pt QRE) and 328 K for 4h.

However, no peaks relate to Li (2θ=36.50°, 52.58°, 65.70°, 77.56° and 88.90°, from the JCPDS database) or Li-Pt alloy (2θ=21.00°, 38.05°, 43.83°, 58.53° and 72.77°, from the JCPDS database), indicating no crystal Li exists in the deposit. The peaks at about 2θ=20.35°, 38.90°, 40.69°, 47.67°, 69.13° and 83.69°, have a left shift compared to that of Cu-Pt alloy (2θ=20.40°, 39.22°, 41.01°, 47.97°, 69.58° and 84.29°, from the JCPDS database), which can be explained by the insertion of Li atoms into Cu-Pt alloy lattices. Some of deposited Cu atoms formed Cu-Pt alloy with Pt atoms in the substrate, and then part of deposited Li atoms penetrated to the lattice gap of Cu-Pt alloy during codeposition procedure, which increases the lattice interdistance of Cu-Pt alloy. According to Braag diffraction formula, as shown in Equ. 1, the diffraction peaks of Cu-Pt alloy shift to a smaller 2θ as the increasing of interdistance. Similar situation was reported by Friedfeld in the study of codeposition of $CuIn_xGa_{1-x}Se_2$. [28]

$$n\lambda = 2d\sin\theta \qquad \text{Equ. 1}$$

X-ray photoelectron spectroscopy is used to obtain further information about the composition and structure of surface layer due to its ability to distinguish between different oxidation states. Fig. 6 shows detailed XPS spectra of the Li 1s, the Cu 2p1/2 and the Cu 2p3/2 peaks, respectively. A rough compensation for the charging effects was carried out by shifting the energy scale so that the main C 1s peak obtained a binding energy of 284.6 eV. Two peaks were used in order to obtain a satisfactory fit for the Li 1s spectra. The lower energy peak at 55.0 eV is believed to originate from metallic lithium and the peak at 55.9 eV is ascribed to lithium oxide.[29] The Cu 2p3/2 spectrum was fitted with two peaks, Cu at 932.5 eV and CuO at 933.2 eV.[30] The Cu 2p1/2 peak appearing demonstrates existence of the copper oxide. It can be fitted by two peaks. One is at 952.8 eV representing Cu_2O and the other is at 953.8 eV representing CuO. The XPS results show that not only metallic Li and Cu but also their oxides exist in the deposit. The oxides may be introduced owing to the sample exposing to air before putting it into sample room since Li and Cu is oxidized easily in the air. The result of XPS has a good agreement with the results of ICP and XRD.

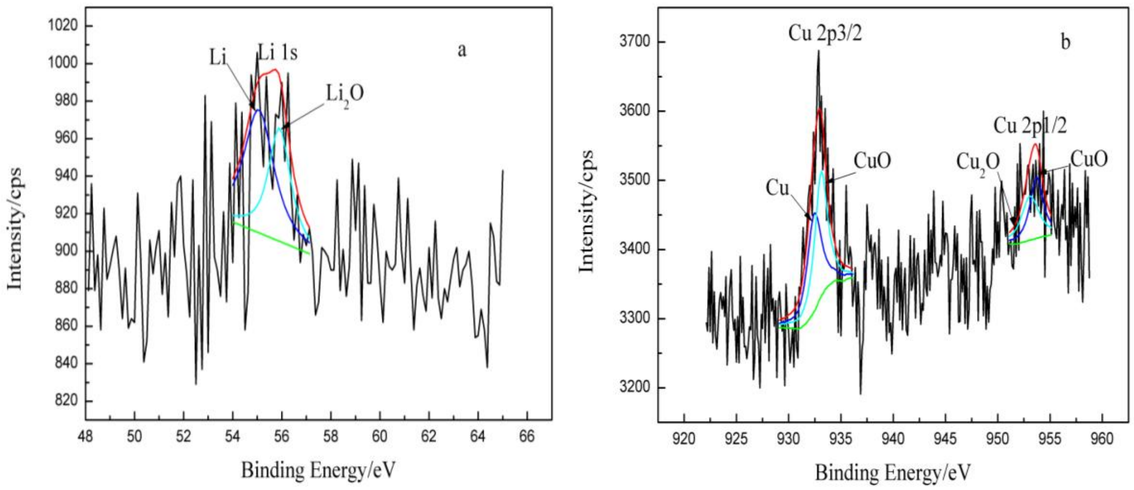

Figure 6. XPS spectra of a) Li 1s and b) Cu 2p3/2 and Cu 2p1/2

The surface morphology of the 76.81at% Li-Cu deposit was smooth and dense, as shown in Fig. 7a. After putting the deposit in air for 2 hours, the colour of deposit changed from black to shine gray, which indicates the 76.81at% Li-Cu deposit is unstable in the air. Cu framework with mesh porous structure, as shown in Fig. 7b, was obtained after dissolving deposited Li of 76.81at% Li-Cu in distilled water. These pores in Cu framework generated at the position where Li deposited, implying the deposited Li distributes uniformly in 76.81at% Li-Cu deposit. This Cu framework is expected to be an active material of anode electrode since the mesh porous structure is shown to be advantageous for anode materials.

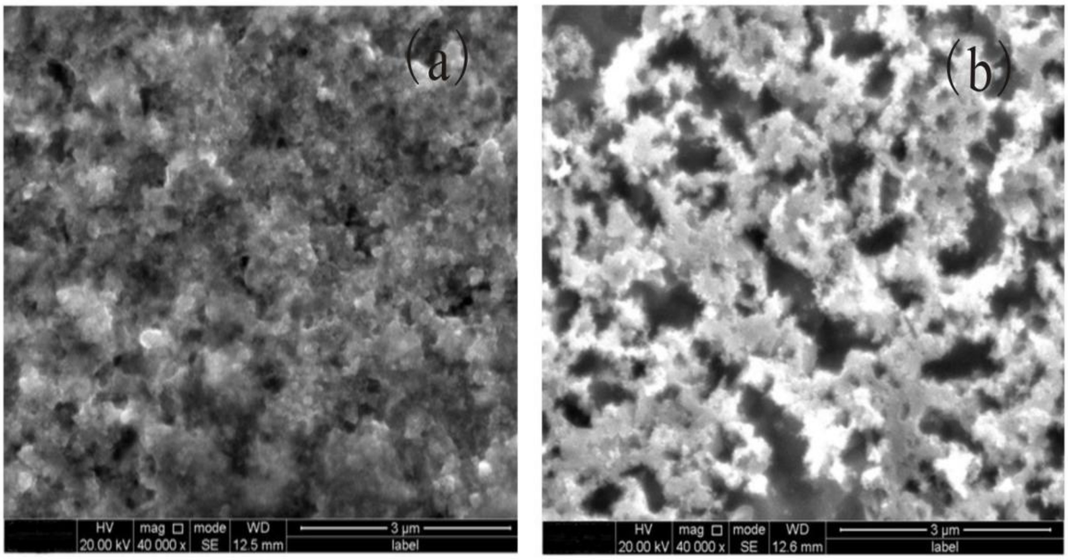

Figure 7. SEM images of a) 76.81at%Li-Cu deposit on Pt WE and b) after dissolving Li of 76.81at%Li-Cu deposit in distilled water.

4. CONCLUSIONS

In the present work, Li-Cu deposits were successfully obtained by electrochemical-codeposition from HMIMOTF ionic liquid containing 0.1M $Cu(CF_3SO_3)_2$ and 1M $LiCF_3SO_3$. At -3.5V and 333 K for 4h, Li atom content in the Li-Cu deposit can reach to 76.81%. Model of induced codeposition shows that the Cu ions and Li ions in electrolyte form insoluble film during induced deposition which doesn't block all the solutions ions from being reduced so that the atom content of Li in Li-Cu deposit increase with the increasing of concentration of Li ions in the electrolyte. XRD result showed that the Li-Cu deposit consisted of amorphous lithium and metallic copper and part of deposited amorphous Li atoms penetrated into the lattice gap of Cu-Pt alloy during codeposition procedure which makes diffraction peaks of Cu-Pt alloy shifting to a smaller 2θ. The surface morphology of 76.81at% Li-Cu was smooth and dense and the deposited Li distributed uniformly in 76.81at% Li-Cu deposit. Cu framework with mesh porous structure was obtained by dissolving deposited Li of 76.81at% Li-Cu in distilled water.

ACKNOWLEDGMENT
This work is supported by Project (No. 51074057) of National Nature Science Foundation of China.

References

1 A. P. Abbott and K. J. Mckenzie. *J. Phys. Chem. Chem. Phys.* 8 (2006) 4265.
2 F. Endres, D. MacFarlane and A. P. Abbott. *Electrodepositon from Ionic Liquid*, John Wiley and Sons Ltd. Wiley-VCH (2008)
3 P. Y. Chen and C. L. Hussey. *J. Elecreochimica Acta*, 52 (2007) 1857.
4 Y. T. Hsieh, T. I. Leong, C. C. Huang, C. S. Yeh and I. W. Sun. *J. Chem. Commun.* 46 (2010) 484.
5 A. Lisenkov, M. L. Zheludkevich and M. G. S. Ferreira. *J. Electrochem.Commun.* 12 (2010) 729.
6 P. Y. Chen, M. J. Deng and D. X. Zhuang. *J. Electrochimica Acta*. 54 (2009) 6935.
7 S. Z. E. Abedin, A. Y. Saad, H. K. Farag, N. Borisenko, Q. X. Liu and F. Endres. *J. Electrochimica Acta*. 52 (2007) 2746.
8 S. Z. E. Abedin, E. M. R. Hempelmann, H. Natter and F. Endres. *J. Electrochem. Commun*. 7 (2005) 1111.
9 A. Bakkar and V. Neubert. *J. Electrochem. Commun.* 9 (2007) 2428.
10 R. Al-Salman and F. Endres. *J. Mater. Chemistry.* 19 (2009) 7228.
11 H. Sano, H. Sakaebe and H. Matsumoto. *J. Power Sources*. 196 (2011) 6663.
12 C. A. Paddon and R. G. Compton. *J. Phys. Chem. C. Lett.* 111 (2007) 9016.
13 C. M. Park, J. H. Kim, H. Kim and H. J. Sohn. *J. Chem. Soc. Rev*. 39 (2010) 3115.
14 G. B. Appetecchi, F. Alessandrini, R. G. Duan, A. Arzu and S. Passerini. *J. Power Sources*. 101 (2001) 42.
15 T. Tatsuma, M. Taguchi and N. Oyama. *J. Electrochimica Acta*. 46 (2001) 1201.
16 Y. Fu, X. Ma, Q. Yang and X. Zong. *J. Mater. Lett.* 57 (2003) 1759.
17 M. Ishikawa, S. Machino and M. Morita. *J. Electroanal. Chem.* 473 (1999) 279.
18 H. Ota, K. Shima, M. Ue and J. Yamaki. *J. Electrochimica Acta*. 49 (2004) 565.
19 S. Zhang. *J. Power Sources*. 162 (2006) 1379.
20 K. D. Kepler, J. T. Vaughey and M. M. Thackeray, *J. Electrochem. and Solid-State Lett.* 2 (1999) 307.
21 C. F. Old and P. Trevena. *J. Met. Sci.* 15 (1981) 281.
22 O. A. Lambri, J. I. Pe´rez-Landaza´bal, A. Pen˜aloza, O. Herrero, V. Recarte, M. Ortiz and C. H. Wo¨rner. *J. Mater. Resear. Bull.* 35 (2000) 1023.
23 H. J. Wang, J. M. Wang, W. B. Fang, H. Wan, L. Liu, H. Q. Lian, H. B. Shao, W. X. Chen, J. Q. Zhang and C. N. Cao. *J. Electrochem. Commun.* 12 (2010) 194.
24 E. Peled, D. Golodnitsky, G. Ardel and V. Eshkenazy. *J. Electrochimica Acta*. 40 (1995) 2197.
25 C. S. Cheng, F. M. Wang and J. Rick. *J. Int J Electrochem Sc*. 9 (2012) 8676.
26 T. C. Frankiln. *J. Sur. and Coat. Tech.* 82 (1996) 65.
27 Z. M. Tu. *Mechanism and Technology of Electroplating of Alloys*, National Defense Industry Publisher, Beijing, 1993.
28 R. Friedfeld, R. P. Ra!aelle and J. G. Mantovani. *J. Sol. Energ. Mat. Sol. Cell. 58 (1999) 375.*
29 M. L.Shek, J. Hrbek, T. K.Sham and G. Q. Xu. *J. Surf. Sci.* 324 (1990) 234.
30 N. S. McIntyre and M. G. Cook. *J. Anal. Chem.* 47 (1975) 2208.